

Home Search Collections Journals About Contact us My IOPscience

Highly efficient electrophosphorescence devices based on iridium complexes with high efficiency over a wide range of current densities

This article has been downloaded from IOPscience. Please scroll down to see the full text article.

2008 J. Phys. D: Appl. Phys. 41 245101

(http://iopscience.iop.org/0022-3727/41/24/245101)

View the table of contents for this issue, or go to the journal homepage for more

Download details:

IP Address: 159.226.165.151

The article was downloaded on 10/09/2012 at 01:42

Please note that terms and conditions apply.

J. Phys. D: Appl. Phys. 41 (2008) 245101 (6pp)

Highly efficient electrophosphorescence devices based on iridium complexes with high efficiency over a wide range of current densities

Liying Zhang^{1,2}, Ping Chen³, Bin Li¹, Ziruo Hong¹ and Shiyong Liu³

E-mail: lib020@ciomp.ac.cn (B Li) and syliu@mail.jlu.edu.cn (S-Y Liu)

Received 28 May 2008, in final form 11 September 2008 Published 25 November 2008 Online at stacks.iop.org/JPhysD/41/245101

Abstract

Three new luminescent cyclometalated iridium (III) complexes are successfully synthesized. The cyclometalated ligand used here is 2-(2-fluorophenyl)-benzothiazole (F-BT). The auxiliary ligands are acetylacetone (acac), 1,1,1-trifluoroacetylaceton (3F-acac), 1,1,1,5,5,5-hexafluoroacetylacetone (6F-acac), respectively. All complexes exhibit bright photoluminescence at room temperature. Organic light-emitting diodes are fabricated by doping the iridium (III) complexes in 4, 4'-N, N'-dicarbazole-biphenyl (CBP), and the device characteristics are investigated. Among these devices, the performances of the optimized devices based on 1 at high current density are among the best reported for devices with iridium (III) complexes as emitters. EL efficiencies show weak dependence on doping concentration and current density. The optimized device exhibits a peak current efficiency of 28.5 cd A⁻¹ and a power efficiency of 11.2 lm W⁻¹, respectively, at 20 mA cm⁻², an efficiency of 22.7 cd A⁻¹ at 100 mA cm⁻², 80% of the maximum, can be achieved. Short triplet decay time of 1 measured in solid films is supposed to be responsible for the minor loss in EL efficiency, which suggests depressed triplet-triplet annihilation and site saturation of the phosphor. Efficient exciton formation on the molecules of 1 by direct charge trapping and confinement within the emissive layer also make for outstanding electrophosphorescent performances.

1

1. Introduction

The efficiency of organic light-emitting diodes (OLEDs) has been dramatically improved by the use of phosphorescent complexes [1–6]. Strong spin–orbit coupling induced by the central heavy metal atom allows mixing of symmetric and asymmetric electronic states of organic molecules, and thus triggers radiative relaxation of triplet excitons, which populate 3/4 of the total excitons generated by charge recombination. Therefore, an internal quantum efficiency of 100% can be achieved by harnessing both singlet and triplet excitons [2,7].

The main drawback of phosphorescent materials for OLED applications is the relatively long exciton decay time, which is responsible for saturation of emissive phosphor sites and triplet-triplet (T-T) annihilation [8–10]. As a result, the peak electrophosphoresence efficiency typically occurs at low current densities ($J < 0.1 \,\mathrm{mA\,cm^{-2}}$), necessitating the minimization of leakage currents that do not contribute to luminescence [11]. The significant roll-off of efficiency with current holds back the development of passive matrix OLEDs based on phosphorescent materials. Short triplet lifetime of a phosphorescent material is crucial for high electroluminescence (EL) efficiency at high current, which

¹ Key Laboratory of Excited State Processes, Changchun Institute of Optics, Fine Mechanics and Physics, Changchun 130033, People's Republic of China

² Graduate School of the Chinese Academy of Sciences, Chinese Academy of Sciences, Beijing 100039, People's Republic of China

³ State Key Lab of Integrated Optoelectronics, Jilin University, Changchun 130023, People's Republic of China

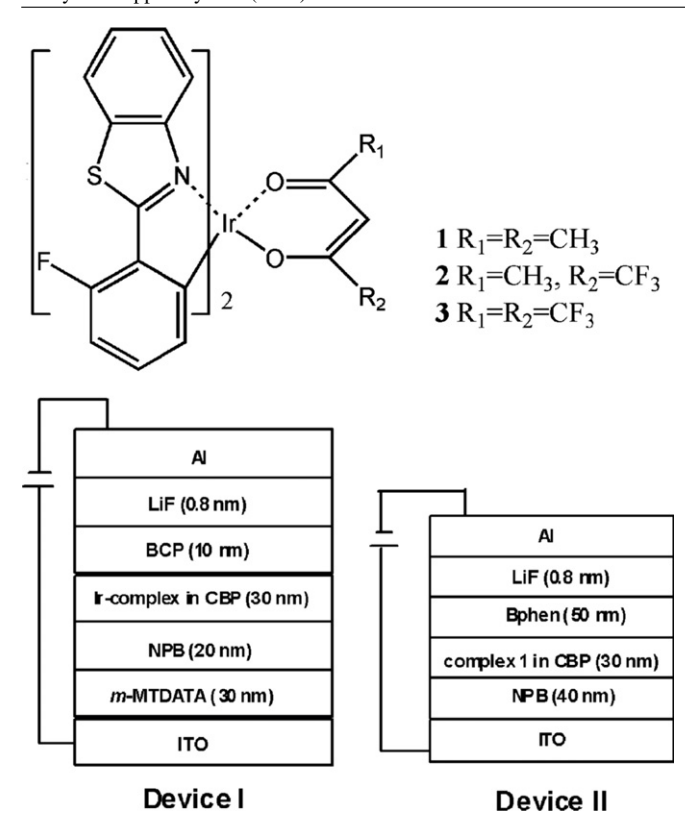


Figure 1. Chemical structure of **1–3** and the configuration of devices.

would enable application of phosphorescent materials for passive matrix displays. Therefore, it is highly desirable to obtain phosphors with short lifetimes. Among those phosphors, iridium (III) complexes have attracted considerable interest because of their excellent EL performances, including very high efficiency and operational stability [12–18]. Both the EL efficiency and the emissive wavelength of the devices based on iridium (III) complexes are greatly affected by the organic ligands [19–21]. Until now, several groups have reported highly efficient iridium (III) complexes consisting of fluorine in the cyclometalated ligands [22–24]. Unfortunately, most of them have a long lifetime (>1 μ s). To this end, we attempted to synthesize a new cyclometalated ligand F-BT and three novel iridium (III) complexes (F-BT)₂Ir(acac) (1), (F-BT)₂Ir(3Facac) (2) and (F-BT)₂Ir(6F-acac) (3), which are shown in figure 1. All complexes exhibit bright photoluminescence (PL) at room temperature. EL devices are fabricated by doping the iridium (III) complexes in 4, 4'-N, N'-dicarbazole-biphenyl (CBP), and the device characteristics are studied. Among these iridium (III) complexes, 1 has a short decay time of $0.85 \,\mu s$. EL devices based on 1 doped CBP films with the configuration of II exhibit high efficiency over a wide range of current. At 20 mA cm⁻², the peak current efficiency of 28.5 cd A⁻¹, corresponding to the power efficiency of $11.2 \,\mathrm{lm}\,\mathrm{W}^{-1}$, is achieved. Moreover, increasing current density to 100 mA cm⁻², EL efficiency of 22.7 cd A⁻¹ can still be obtained as high as 80% of the maximum efficiency. We believe that this good performance is attributable mainly to the short phosphorescent lifetime of 1. Another important factor to enhance the device performances is efficient exciton

formation on the molecules of **1** by direct charge trapping and confinement within the emissive layer.

2. Experimental details

The ligand F-BT, and the corresponding complexes 1-3, were synthesized separately according to synthesis procedures [17, 25]. Both ligand and complexes were characterized by ¹H NMR, IR and elemental analysis. Detailed characterization for complex 1: ¹H NMR (CDCl₃, 500 MHz) δ [ppm]: 1.76 (s, 6 H), 5.13 (s, 1H), 6.13 (d, J = 7.5 Hz, 2 H), 6.55 (d, $J = 8.5 \,\mathrm{Hz}, 2 \,\mathrm{H}$), 6.66 (d, $J = 7.0 \,\mathrm{Hz}, 2 \,\mathrm{H}$), 7.47 (m, 4 H), 7.94 (m, 2 H), 8.11 (m, 2 H). IR (KBr, cm⁻¹): 1707 (C=O), 422 (Ir-O). Anal. Calcd for C₃₁H₂₁F₂IrN₂O₂S₂: C 49.78, H 2.83, N 3.74 found: C 49.54, H 3.10, N3.90. Detailed characterization for complex 2: ¹H NMR (CDCl₃, 500 MHz) δ [ppm]: 1.89 (s, 3 H), 5.52 (s, 1 H), 6.13 (d, J = 7.3 Hz, 2 H), 6.60 (d, J = 10 Hz, 2 H), 6.68(d, J = 8.0 Hz, 2 H), 7.50 (m, 4 H), 7.91 (m, 2 H), 8.27 (m, 2 H). IR (KBr, cm⁻¹): 1703 (C=O), 425 (Ir–O). Anal. Calcd for C₃₁H₁₈F₅IrN₂O₂S₂: C 46.43, H 2.26, N 3.49 found: C 46.62, H 2.04, N 3.31. Detailed characterization for complex 3: ¹H NMR (CDCl₃, 500 MHz) δ [ppm]: 5.52 (s, 1 H), 6.13 (d, J = 7.3 Hz, 2 H), 6.60 (d, $J = 10 \,\text{Hz}$, 2 H), 6.68(d, $J = 8.0 \,\text{Hz}$, 2 H), 7.50 (m, 4 H), 7.91 (m, 2 H), 8.27 (m, 2 H). IR (KBr, cm⁻¹): 1691 (C=O), 424 (Ir–O). Anal. Calcd for C₃₁H₁₅F₈IrN₂O₂S₂: C 43.50, H 1.77, N 3.27 found: C 43.25, H 1.94, N 3.50. The highest occupied molecular orbital (HOMO) and the lowest unoccupied molecular orbital (LUMO) energy levels of 1 were determined by cyclicvoltammetry. The EL devices with the configuration: ITO/4,4',4"-tris[3-methyl- phenylphenylaminoltriphenylamine (m-MTDATA) (30 nm)/4,4′-bis[N-(1naphthyl)- N-phenylamino]biphenyl (NPB) (20 nm)/x wt% Ir-complex doped in CBP (30 nm)/BCP (10 nm)/tris(8hydroxy-quinoline)aluminium (Alq₃) (30 nm)/LiF (0.8 nm)/Al (I) and ITO/NPB (40 nm)/x wt% 1 doped in CBP (30 nm)/4,7diphenyl-1,10-phenanthroline (Bphen) (50 nm)/LiF (0.8 nm)/ Al (II), which are demonstrated in figure 1, are fabricated. The EL devices were fabricated by high-vacuum ($\leq 8 \times 10^{-5} \, \text{Pa}$) thermal deposition of the materials onto a clean glass that was pre-coated with a layer of indium tin oxide (ITO). Prior to use, the ITO surface was cleaned by sonication in detergent solution, water and ethanol sequentially. After being blown dry with nitrogen, the ITO substrates were treated with oxygen plasma for 1 min before being loaded into the vacuum chamber. LiF/Al were used as the electron-transporting layer and the cathode, respectively. The thicknesses of the deposited layers and the evaporation speed of the individual materials were monitored in vacuo with quartz crystal monitors. The UV-visible absorption spectrum was obtained on a shi-madzu-UV-3101 scanning spectraphotometer. Steady state PL spectra were measured with a RF-5301Pc spectrofluorophotometer. The PL decays of these complexes in solution and 1 at different concentrations in CBP films excited by laser pulse at wavelength 355 nm were measured by a quanta ray DCR-3 pulsed Nd: YAG laser system. EL spectra of these devices were measured by a PR650 spectrascan spectrometer. The luminance-current density-voltage characteristics were

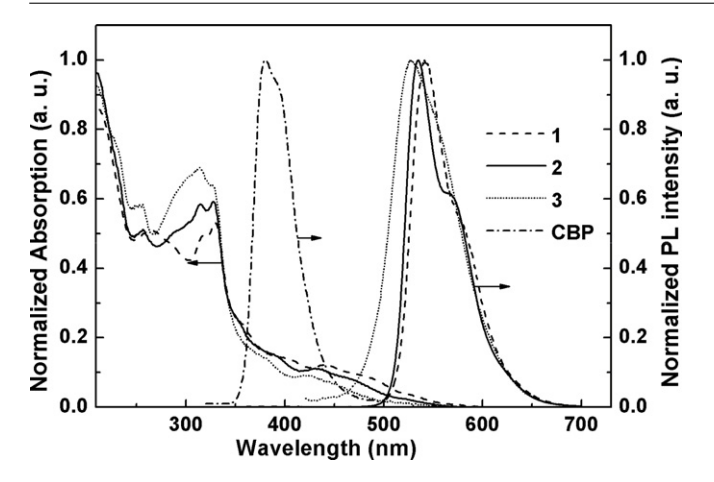


Figure 2. Absorption and emission spectra of complexes **1–3**, and emission spectrum of CBP in film.

recorded simultaneously with the measurement of EL spectra by combining the spectrometer with a Keithley 2400 source meter. All measurements were carried out in air at room temperature.

3. Result and discussion

3.1. Photophysical properties

In order for these iridium (III) complexes to be useful as phosphors EL devices, strong spin-orbit coupling must be present to efficiently mix the singlet and triplet excited states. Clear evidence for mixing of the singlet and triplet excited states are seen in both the absorption and the emission spectra of the complexes. Absorption and emission spectra of the complexes were measured in dichloromethane solutions with a concentration $1.0 \times 10^{-4} \text{ mol L}^{-1}$ at 298 K. Figure 2 shows a comparison of absorption, excitation and emission spectra of complexes 1-3 and the emission spectrum of CBP in film, and the relevant data are summarized in table 1. For these complexes, intense multiple absorption bands appearing in the ultraviolet part of the spectrum between 250 and 330 nm are assigned to the spin-allowed $\pi - \pi^*$ transitions of the F-BT ligand. The broad weak absorption bands at 460 and 520 nm are assigned to the transitions from the ground state to the singlet metal-ligand-charge-transfer (¹MLCT) and triplet MLCT (³MLCT) excited states [6, 26]. The intensity of the ³MLCT transition is close to that of ¹MLCT, suggesting that the ³MLCT transition is strongly allowed by an effective mixing of singlet-triplet with higher lying spin-allowed transitions on the cyclometalated ligand [6]. This mixing is facilitated by the strong spin-orbit coupling of the iridium centre. In addition, the similarity of the ³MLCT energies for these complexes is unsurprising, since all three complexes have similar ³MLCT states involving the same fragment of the F-BT ligand.

The complexes of **1** and **2** show similar structural features in their emission spectra, with emission maximum at ca 542 nm, 534 nm and a shoulder at ca 580 nm, 570 nm, respectively. Whereas, in comparison with the complexes **1** and **2**, the emission spectrum of **3** is broad, which exhibits a broad band centring at 528 nm and the shoulder peak becomes

Table 1. Physical parameters for complexes 1–3.

Complex	Absorption $\lambda_{\max}(nm)^a$	Emission $\lambda_{max}(nm)^a$	τ (μs)
1	264, 316, 328, 402, 440, 477, 525	542, 580	0.85
2	257, 314, 328, 386, 434, 467, 525	534, 570	2.27
3	251, 310, 328, 384, 425, 450, 520	528	4.8

very weak. The emission spectra of complexes 2 and 3 are slightly blue-shifted in comparison with that of 1, which is the result of the introduction of -F substitute, a strong electron-withdrawing substitute, into the acac moiety that is considered to decrease the HOMO level. Finally, the radiative lifetimes of these complexes are measured and fall in the range $0.85-4.8 \,\mu s$. Among these complexes, a significant feature of 1 is the short lifetime of the triplet excited state, which is $0.85 \,\mu s$.

3.2. EL properties

To investigate the EL properties of these complexes, several devices based on different iridium (III) complexes as an emitter were fabricated. First, the multilayer device I: ITO/ m-MTDATA (30 nm)/NPB (20 nm)/ x wt% Ir-complex doped in CBP (30 nm)/BCP (10 nm)/Alq₃ (30 nm)/LiF (0.8 nm)/Al was fabricated; m-MTDATA is used as the hole-injection layer, NPB is the hole-transporting and electron-blocking layer, and meanwhile BCP and Alq3 are employed as the hole-blocking layer and the electron-transporting layer, respectively. Considering the triplet energy of iridium complexes (ca 2.25 eV) which were obtained by testing their emission spectra at 77 K, CBP is used as the host because of its high triplet energy (2.56 eV) which should be responsible for the efficient energy transfer and its proven performances as host for iridium complexes [27]. To optimize the device efficiency, a concentration dependence experiment was carried out in the range 6–14 wt%. The devices based on 1 and 2 have intense vellow emission originating from the iridium complexes, but no emission was detected from the devices based on 3. The results of the complexes TGA show that the complex tends to thermally decompose at relatively low temperature as the increase in fluorine in the ancillary ligand. Among these three complexes, the thermo-stability of complex 3 is the worst, so 3 is prone to decomposition in the deposition process. This result can decrease its film-forming property, and then make the luminescent performance of the devices based on 3 suffer severely. The current density-brightness characteristics for 1 and 2 based devices with a configuration of I are displayed in figures 3 and 4, respectively, and current efficiency versus current density characteristics for 1 and 2 are shown in figure 5. Among these devices, the device based on complex 1 with the concentration of 12 wt% demonstrates the best performance with a maximum brightness 38000 cd m⁻² at 20 V, and a current efficiency 27.8 cd A^{-1} at 1.1 mA cm^{-2} . This is in agreement with the highest PL quantum efficiency of complex 1. The highest brightness and current efficiency achieved from the devices based on $\bf 2$ are 27 000 cd m⁻² at 17 V and 8.8 cd A⁻¹ at $3.7 \,\mathrm{mA \, cm^{-2}}$. Furthermore, from figure 5, we found that the efficiency based on complex 1 shows weak roll-off at high

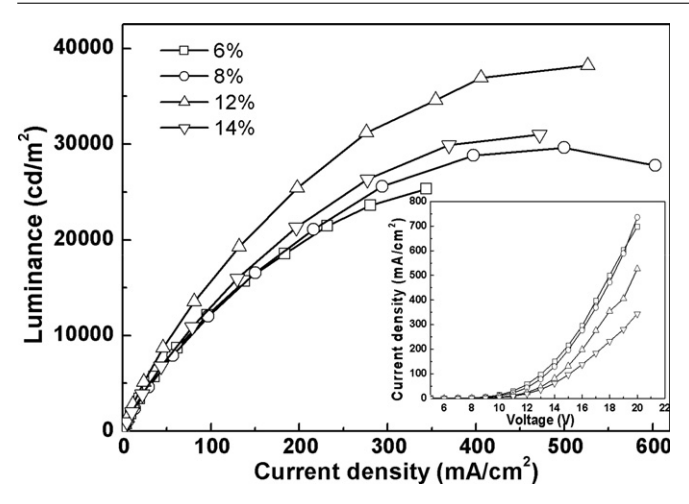


Figure 3. Current density–brightness characteristics for **1** based devices with configuration of I. Inset: current–density versus voltage curves.

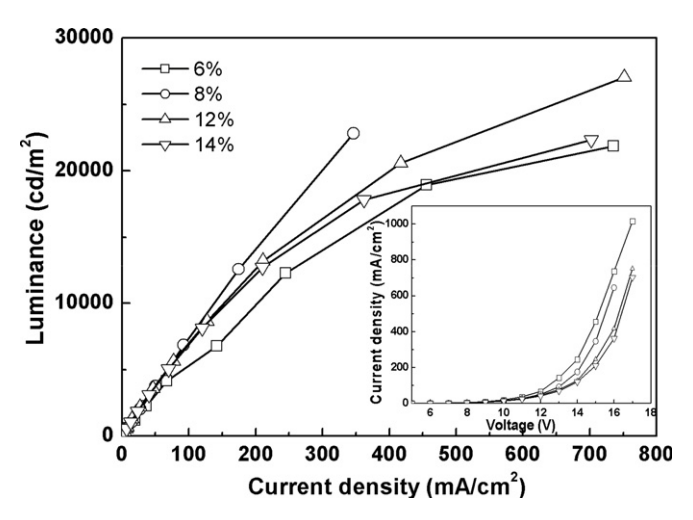


Figure 4. Current density—brightness characteristics for **2** based devices with configuration of I. Inset: current—density versus voltage curves.

current density, while the efficiency of **2** demonstrated a clear decrease with the increasing current. In the same devices configuration, complex **1** exhibits better performance at high current. We guess that the better performance of **1** is partly attributable to the relatively shorter lifetime which reduces the severity of the T–T annihilation.

In order to confirm our suggestion, only complex 1 was subjected to further studies. Another device II with the structure of ITO/NPB (40 nm)/x wt% 1 doped in CBP (30 nm)/Bphen (50 nm)/LiF (0.8 nm)/Al was also fabricated, in which 1 doped CBP host with mass ratios of 6–14 wt% acts as light-emitting layer. Bphen is used as the electron-transporting layer. Figure 6 shows current efficiency versus current density of the devices at different doping concentrations. The efficiency of all devices first increased rapidly and then decreased very slowly with increasing current density. Typical EL characteristics of the devices were summarized in table 2. For all devices, the efficiencies at the current density of $20 \text{ mA} \text{ cm}^{-2}$ are almost equal to the maximum efficiencies.

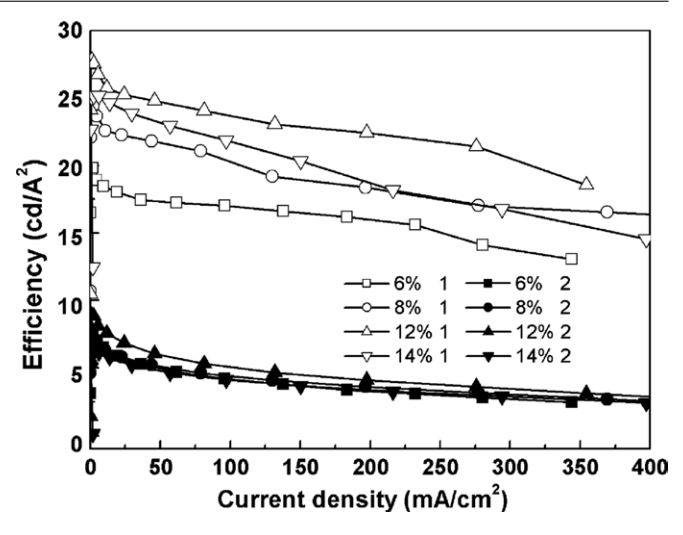


Figure 5. Current efficiency versus current density characteristics for 1 and 2 based devices with the configuration of I.

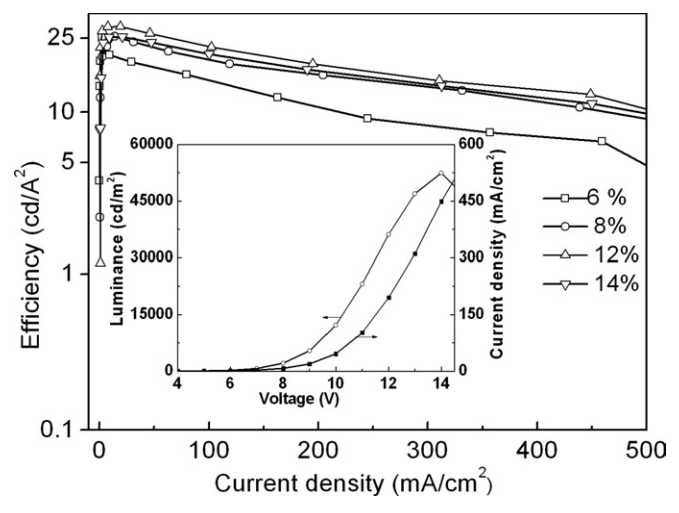


Figure 6. Current efficiency versus current density characteristics for **1** based devices with configuration of II. Inset: current density–brightness–voltage curves of the optimized device based on 12 wt% **1** in CBP.

Even at high current density of 100 mA cm⁻², the efficiencies remain higher than 60% of the peak values. Among the four devices, the one with 12 wt% 1 in CBP offers the highest EL efficiency. This device shows very high efficiency at high current. When current density increases to 20 mA cm⁻², a peak current efficiency of 28.5 cd A^{-1} and a power efficiency of 11.2 lm W⁻¹ are achieved, and a maximum brightness of 52 800 cd m⁻² is recorded at a current density of 450 mA cm⁻², as shown in the inset of figure 6. A high efficiency of $22.7 \operatorname{cd} A^{-1}$ with a luminance of $22\,000 \operatorname{cd} m^{-2}$ can still be obtained at a high current density of 100 mA cm⁻², 80% of the maximum efficiency, and even at 400 mA cm⁻² the efficiency remains 17.1 cd A⁻¹. These values gained at high current density are significantly improved compared with the previous reports employing iridium (III) complexes as emitters in OLEDs [2, 4]. The results show that T–T annihilation is not severe owing to the short lifetime of the 1 excitons. Moreover, the direct charge trapping by 1 molecules is also a main factor

Table 2. Typical EL characteristics of the devices II with different doping 1 concentrations.

Concentration (%)	$\tau^{\rm a}$	$B_{ m max}^{ m b}$	$\eta_{\mathrm{max}}^{\mathrm{c}}$	$\eta^{ m d}$	η^{e}	$\eta^{ m f}$
6	1.26	32 201	25.1	19.3	15.2	7.3
8	1.15	48 260	25.5	24.9	18.6	12.5
12	1.10	52 800	28.5	28.5	22.7	17.1
14	1.08	45 850	25.4	25.3	20.8	12.4

- ^a Triplet excited state lifetime (μs).
- ^b Maximum brightness (cd m⁻²).
- ^c Maximum current efficiency (cd A⁻¹).
- ^d Current efficiency at 20 mA cm⁻² (cd A⁻¹).
- ^e Current efficiency at 100 mA cm⁻² (cd A⁻¹).
- f Current efficiency at 400 mA cm⁻² [cd A⁻¹].

in enhancing the device performances. These can be inferred from the following analysis.

Table 2 shows the lifetime of 1 triplet at different concentrations in CBP films. By introducing fluorine atoms on the BT ligand, the lifetime of 1 becomes shorter compared with that of $(BT)_2Ir(acac)(1.8\,\mu s)$ [16]. From table 2, it is worth noting that triplet decay of 1 is almost independent of doping concentration, and the maximum difference between the samples is merely $0.18\,\mu s$. Consequently, concentration quenching effects arising from T-T annihilation between different complex molecules (at high current densities) are not serious even at high doping level. Furthermore, the lifetime of host CBP is $0.5\,\mu s$, the lifetime difference between the host and the dopant is merely $0.35\,\mu s$, which is closely matched and enough to reduce the extent of the saturation of the dopant triplet emissive sites [1]. Hence the efficiencies of the devices do not exhibit a steep roll off as the current density is raised.

The mechanism of the EL devices II was also discussed. The considerable overlap between the fluorescence of CBP and the ¹MLCT absorption of **1**, as shown in figure 3, indicates that Förster energy transfer from the singlet in the CBP host to the ¹MLCT state of **1** is possible. On the other hand, for PL spectra of 1 doped CBP films, as shown in figure 7(a), emission from CBP becomes weak with the increasing doping concentration, whereas, 14 wt% doping concentration is still not enough to fully quench CBP emission. This implies Förster energy transfer from the host (CBP) to the guest 1 is incomplete due to the relatively weak ¹MLCT absorption. In contrast to the case of PL, no CBP emission is observed from the EL devices even at low doping concentration of 6 wt%, as shown in figure 7(b). The absence of CBP emission suggests direct charge trapping and recombination with opposite charge carriers on 1 dopant. According to the energy level alignment in figure 8, the charge-trapping mechanism is favourable, since the HOMO and LUMO levels of 1 are 5.8 eV and 3.42 eV, respectively, lying between the band gap of CBP, which meets the requirement for efficient carrier trapping [28]. The LUMO of 1, 0.5 eV higher than that of CBP, may behave as deep electron traps in CBP, enabling effective electron transport therein. Its HOMO level, which is 0.2 eV lower than CBP, also eases hole injection from NPB to CBP. So the direct charge trapping is likely to be the dominant process in the EL devices. Meanwhile, efficient charge trapping of complex 1 is supported by the current density versus voltage (J - V)

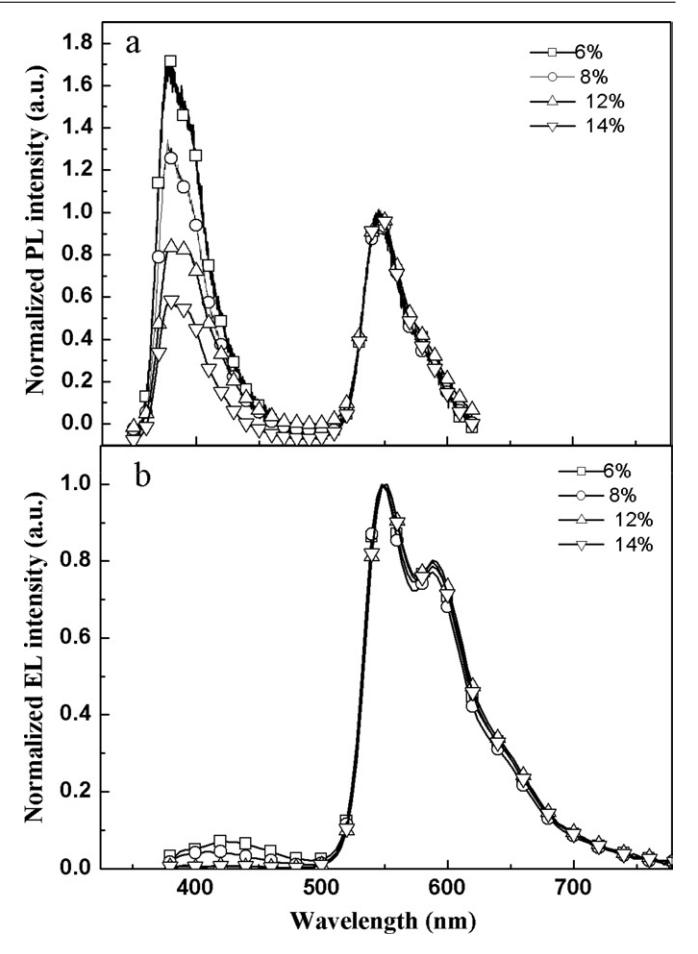


Figure 7. (a) PL of thin films and (b) EL spectra of devices II with different 1 concentrations in CBP.

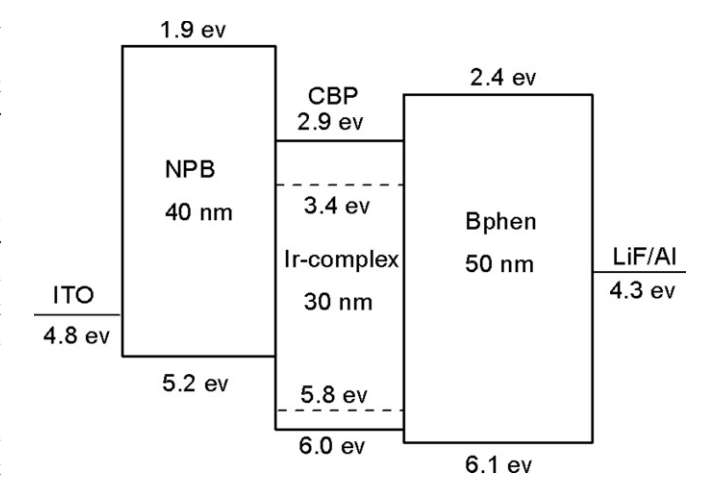


Figure 8. The proposed energy level diagram of devices II.

characteristics of the EL devices based on 1 with different doping levels, as illustrated in the inset of figure 3. We can see that the J-V characteristic curves shift gradually to higher voltage with increasing doping concentration, suggesting that the trapping effect of the iridium (III) complexes basically decreases the carrier transport mobility.

EL spectra based on device II are dominated by Ir-complex emissions, a main band at $550\,\mathrm{nm}$ and a secondary band at

587 nm, which shows a redshift of \sim 8 nm compared with its PL spectrum, indicating negligible aggregation effect of the dopant [29]. At concentrations of 6 wt% and 8 wt%, a slight blue emission at 450 nm from NPB is observed, and disappears as the doping concentration is increased to 12 wt% or higher. Such a phenomenon is direct evidence for chargetrapping mechanism. Since hole injection from the NPB HOMO into the CBP HOMO is energetically unfavourable, when the dopant concentration is low, accumulated holes in the NBP layer can recombine with the electrons injected from the emissive layer, resulting in NPB emission in addition to exciton formation at 1. With increasing doping concentrations, more and more electrons can be intercepted and trapped by 1 and the contribution from NPB decreased. At 1 concentration higher than 12 wt%, no electrons are injected into the NPB layer, so the NPB emission disappears. Another important feature in our devices is that bright white EL emission (Commission International de L'Eclairage chromaticity coordinates at X = 0.34, Y = 0.33) is observed at low concentration, suggesting that the combination of complex 1 with blue emitters may result in efficient white OLEDs.

The decrease in NPB emission with increasing dopant concentration is also a hint for the shift of the recombination zone in the EL devices. Due to the similar HOMO level of Ir-complex and CBP, holes injection barrier from NPB to CBP cannot be completely removed with the presence of 1. That is the reason for high turn-on voltage Therefore, significant charge accumulation at NPB/CBP interface may occur at low dopant concentration, resulting in exciton accumulation, which accounts for the relatively low EL efficiency of 6% doped device. increasing dopant concentration, the charge and exciton accumulation can be eased, and recombination zone extends deeply into the doped CBP layer. That means the exciton and charge densities at a given current are lowered, reducing the possibility of non-radiative decay induced by both exciton-exciton and exciton-polaron interaction. Therefore, EL efficiency is improved with increasing dopant concentration.

4. Conclusions

We have systematically investigated the photophysical and electroluminescent properties of three new iridium complexes. All the complexes exhibit a bright phosphorescent emission at ambient conditions. High-performance yellow-emitting devices based on 1 and 2 were fabricated. Among the devices in this study, the 1 based device with the configuration II shows the best performance. Due to the short triplet exciton lifetime of 1, high efficiency can be maintained at high current density with negligible quenching effects of either the T–T annihilation or saturation of the excited state. Such an outstanding performance of the devices based on 1 reveals their potential applications for passive matrix (as well as active matrix) displays.

Acknowledgments

The authors are grateful for the financial support of the One Hundred Talents Project from the Chinese Academy of Sciences and the NSFC (Grant No. 20571071).

References

- [1] Baldo M A, Lamandky S, Burrows P E, Thomposon M E and Forrest S R 1999 *Appl. Phys. Lett.* **75** 4
- [2] Adachi C, Baldo M A, Forrest S R, Lamansky S, Thompson M E and Kwong R C 2001 Appl. Phys. Lett. 78 1622
- [3] Duan J P, Sun P P and Cheng D H 2003 Adv. Mater. 15 224
- [4] Su Y J, Huang H L, Li C L, Chien C H, Tao Y T, Chou P T, Datta S and Liu R S 2003 Adv. Mater. 15 884
- [5] Peng H J, Zhu X L, Sun J X, Yu X M, Wong M and Kwork H S 2006 Appl. Phys. Lett. 88 033509
- [6] Lamansky S, Djurovich P, Murphy D, Abdel-Razzaq F, Lee H E, Adachi C, Burrows P E, Forrest S R and Thomposon M E 2001 J. Am. Chem. Soc. 123 4304
- [7] Baldo M A, O'Brien D F, You Y, Shoustikov A, Sibley S, Thompson M E and Forrest S R 1998 Nature 395 151
- [8] Xie Z H, Liu M W, Wang O Y, Zhang X H, Lee C S, Hung L S, Lee S T, Teng P F, Kwong H L, Zheng H and Che C M 2001 Adv. Mater. 13 1245
- [9] Baldo M A, O'Brien D E, Thompson M E and Forrest S R 1999 Phys. Rev. B 60 14422
- [10] Klessinger M and Michl J 1995 Excited States and Photochemistry of Organic Molecules (Weinheim: VCH)
- [11] Baldo M A and Forrest S R 2000 Phys. Rev. B 62 10958
- [12] Wang Y, Herron N, Grushin V V, LeCloux D and Petrov V 2001 Appl. Phys. Lett. 79 449
- [13] Calogero G, Giuffrida G, Serroni S, Ricevuto V and Campagna S 1995 *Inorg. Chem.* **34** 541
- [14] Neve F, Crispini A, Campagna S and Serroni S 1999 *Inorg. Chem.* 38 2250
- [15] Adachi C, Baldo M A, Forrest S R and Thompson M E 2000 Appl. Phys. Lett. 77 904
- [16] Tsuboyama A et al 2003 J. Am. Chem. Soc. 125 12971
- [17] Chang W C, Hu A T, Duan J P, Rayabarapu D K and Cheng C H 2004 J. Organomet. Chem. 689 4882
- [18] Zhang X W, Gao J, Yang C L, Zhu L N, Li Z A, Zhang K, Qin J G, You H and Ma D G 2006 J. Organomet. Chem. 691 4312
- [19] Yang C H, Tai C C and Sun L W 2004 J. Mater. Chem. 14 947
- [20] Zhang X, Yang C, Chen L and Qin J 2006 Chem. Lett. 35 72
- [21] Grushin V V, Herron N, LeCloux D D, Marshall W J, Petrov V A and Wang Y 2001 Chem. Commun. 1494
- [22] Gong X, Robinson M R, Ostrowki J C, Moses D, Bazan G C and Heeger A J 2002 Adv. Mater. 14 581
- [23] Laskar I R and Chen T M 2004 Chem. Mater. 16 111
- [24] Yang C H, Su W S, Fang K H, Wang S P and Sun I W 2006 Organomet. 25 4514
- [25] Thomas K R, Velusamy M, Lin J T, Chien C H, Tao Y T, Wen Y S, Hu Y H and Chou P T 2005 Inorg. Chem. 44 5677
- [26] Schaffner-Hamann C, Zelewsky A, Barbieri A, Barigelleti F, Muller F, Riehl J P and Neels A 2004 J. Am. Chem. Soc. 126 9339
- [27] Yersin H 2004 Top. Curr. Chem. 241 1 Hay P J 2002 J. Phys. Chem. A 106 1634
- [28] Shoustikov A A, You Y J and Thompson M E 1998 *IEEE J. Sel. Top. Quant.* 4 3
- [29] Ye K, Wang J, Sun H, Liu Y, Mu Z, Li F, Jiang S, Zhang J, Zhang H, Wang Y and Che C M 2005 J. Phys. Chem. B 109 8008